Available online at www.sciencedirect.com

ScienceDirect

Ceramics International 40 (2014) 1993–2004

CERAMICS INTERNATIONAL

www.elsevier.com/locate/ceramint

Halfmetallic ferromagnetism in rare earth nitrides RENs (RE = Gd, Dy, and Ho): A first principles study

R. Rajeswarapalanichamy[a],*, A.T. Asvini Meenaatci[a], K. Iyakutti[b]

[a]Department of Physics, N.M.S.S.V.N College, Madurai, Tamilnadu 625019, India
[b]Department of Physics & Nanotechnology, SRM University, Chennai, Tamilnadu 603203, India

Received 14 April 2013; received in revised form 21 June 2013; accepted 21 July 2013
Available online 27 July 2013

Abstract

The structural, electronic, elastic and magnetic properties of three rare earth nitrides (RENs: RE = Gd, Dy, Ho) are investigated by first principles calculation using Vienna ab-initio simulation code (VASP). At ambient pressure all the three nitrides are stable in the ferromagnetic state (FM) with cubic NaCl(B1) structure. The calculated lattice parameters are in good agreement with experimental and other theoretical values. Electronic structure reveals that these materials are half metallic ferromagnets at normal pressure. A pressure induced structural phase transition from NaCl to wurtzite phase in GdN at 18.2 GPa and from NaCl to CsCl phase in DyN at 104 GPa and HoN at 138 GPa is also predicted. The half metallicity has been retained in GdN, DyN and HoN even after the phase transition but it vanishes at 73.18 GPa, 118 GPa and 141 GPa respectively. Ferromagnetism is quenched in all the three nitrides at a pressure of 252 GPa (GdN), 242 GPa (DyN) and 236.7 GPa (HoN).

Keywords: Electronic structure; Structural phase transition; Magnetic phase transition; Elastic property

1. Introduction

In recent years, the mono-nitrides of rare earth (RE) compounds have drawn considerable interest among material scientist, due to their structural, transport, magnetic and electronic properties [1]. An accurate description of the electronic structure of RE compounds is a very challenging problem because of their partially filled 4f shells [2]. These partially filled 4f shells are responsible for many of the interesting properties in the rare earth nitrides. The class of the rare earth nitrides (RENs), which belong to mono-pnictide family, have a broad range of behavior, from metallic or semi-metallic to semi-conducting. These materials have high magnetic moment and form a wide range of magnetic structures. There has been speculation in the literature that RENs may form half-metallic ferromagnets [3–4]. Half metallic ferromagnetic materials are a class of materials that have metallic behavior for one type of electron spin (↑) and insulating or semiconducting behavior for the other spin (↓), which leads to complete (100%) spin polarization at the Fermi level. The conductivity of these materials occurs with only one spin channel. The actual introduction for half metallic (HM) ferromagnet is given by Groot et al. in 1983 [5]. Because of the half-metallic property, these materials became strong candidates for applications in spintronic and spin-filtering devices and provide new interest in these materials. The HM behavior regarding the electronic, magnetic and transport properties of these compounds are also discussed by Duan et al. [6]. The class of rare earth nitrides have been studied both experimentally [7–13] and theoretically [14,15] in the past by many researchers. Abdelouahed and Alouani [16] investigated the structural stability of GdN using LDA+U method and also observed a structural phase transition from cubic NaCl to hexagonal phase under high pressure. Similarly, Sanjay Bhajanker and his co-workers [17] analyzed the structural and thermal properties of holmium pnictides using inter-ionic potential theory. A pioneering study of rare earth (RE) pnictides was performed by Hasegawa and Yanase [18]. They treated the partially filled f shells simply as core states with a constrained approach. Larson et.al [15] investigated the electronic structure of rare earth nitrides using the LDSA+U approach and identified GdN, DyN and HoN as semiconductors. On the other

---

*Corresponding author. Tel.: +91 452 2459187; fax: +91 452 2458358.
E-mail address: rajeswarapalanichamy@gmail.com (R. Rajeswarapalanichamy).

0272-8842/$ - see front matter © 2013 Elsevier Ltd and Techna Group S.r.l. All rights reserved.
http://dx.doi.org/10.1016/j.ceramint.2013.07.109

hand Aerts et.al [19] observed half-metallic behavior in GdN and insulating behavior in DyN and HoN. From the above mentioned literatures, it is observed that there are some contradictions in the electronic structure of all the three rare earth nitrides. This motivated us to investigate the structural stability, electronic and elastic properties of rare earth nitrides REN (RE:Gd,Dy,Ho). More over to the best of our knowledge the half-metallic to metallic transition, magnetic phase transition and elastic properties for the normal and high pressure phases of GdN, DyN and HoN have not been reported yet.

In the present paper, the electronic band structure calculations at ambient and high pressures are performed using VASP code. The structural phase transition in gadolinium nitride (GdN), Dysprosium nitride (DyN) and holmium nitride (HoN) are analyzed using the obtained energy and enthalpy values. The elastic constants are calculated using energy strain method. The half metallic to metallic transition is predicted from the electronic structure (Band structure and Density of states) of GdN, DyN and HoN. The charge density distribution is also reported for all these nitrides using VASP code.

2. Theoretical framework

The total energy calculations are performed in the frame work of density functional theory using the generalized gradient approximation (GGA-PBE) [20–22] as implemented in the VASP code [23–25]. Ground-state geometries are determined by minimizing stresses and Hellman-Feynman forces using the conjugate-gradient algorithm with force convergence less than 10^{-3} eV Å^{-1}. Birllouin zone integration is performed with a Gaussian broadening of 0.1 eV during all relaxations. The cutoff energy for plane waves in our calculation is 700 eV. The electronic configurations of Gd, Dy, Ho and N atoms are [Xe] $4f^7\ 5d^1\ 6s^2$ (Z=64), [Xe] $4f^{10}\ 6s^2$ (Z=66), [Xe] $4f^{11}\ 6s^2$ (Z=67) and [He] $2s^2 2p^3$ (Z=7) respectively. The valence electronic configurations chosen in our calculation are $4f^7\ 5d^1\ 6s^2$, $4f^{10}\ 6s^2$, $4f^{11}\ 6s^2$ and $2s^2\ 2p^3$ for Gd, Dy, Ho and N atoms respectively. Birllouin-zone integrations are performed on the Monkhorst-Pack K-point mesh [26] with a grid size of $17 \times 17 \times 17$ for structural optimization. Iterative relaxation of atomic positions is stopped when the change in total energy between successive steps is less than 1 meV/cell. With this criterion, the forces on the atoms are generally less than 0.1 eV/Å. The rare earth nitrides GdN, DyN and HoN considered in the present work crystallize in the NaCl structure with space group symmetry Fm3m at normal pressure. In the unit cell of these nitrides, the rare earth atom is positioned at (0, 0, 0) and nitrogen atom at (1/2, 1/2, 1/2). In order to get more accurate value of the band gap energy for the rock salt (B1) phase, we have used GGA plus on-site coulomb self- interaction correction potential (U^{SIC}). The GGA $+U^{\mathrm{SIC}}$ scheme is more appropriate for systems having strongly correlated d or f electrons.

In the GGA+U^{SIC} method, the strong correlation between localized d or f electrons is explicitly taken into account through the screened effective electron–electron interaction parameter ($U_{\mathrm{eff}} = U^{\mathrm{SIC}} - J$), where U^{SIC} and J denote the coulomb and exchange integrals respectively. To obtain the best agreement with experiment, the present results are obtained with the U^{SIC}=9.20 eV, 9.32 eV and 9.57 eV and J=1.2, 1.21 and 1.25 for GdN, DyN and HoN respectively. The value of U^{SIC} is determined by optimizing the band gap to the experimental value. However, it is found that changing U^{SIC} does not affect the value of lattice constant and bulk modulus.

3. Results and discussion

3.1. Structural stability and ground state properties

The stability of rare earth nitrides RENs (RE=Gd, Dy, Ho) are analyzed by calculating the total energy using VASP code based on density functional theory. The mechanical strength of a solid is determined with the help of its cohesive energy, which determines the strongness of binding between the constituent atoms in a solid. The cohesive energy of a solid is the difference between the total energy per atom of the bulk material at ambient condition and the atomic energies of the atoms belonging to the unit cell of the material

$$E_{\mathrm{coh}}^{\mathrm{REN}} = [E_{\mathrm{atom}}^{\mathrm{RE}} + E_{\mathrm{atom}}^{\mathrm{N}} - E_{\mathrm{total}}^{\mathrm{REN}}] \tag{1}$$

where E_{total}^{REN} is the total energy of the compound at the equilibrium lattice constant and E_{atom}^{RE} and E_{atom}^{N} are the atomic energies of the pure constituent atoms. The cohesive energies for rare earth metals (REs) and their nitrides (RENs) are shown in Fig. 1. From Fig. 1, it is observed that the cohesive energies of these nitrides are higher than that of the host elements. It is also observed that, GdN owing to its highest cohesive energy is the most stable one among the considered nitrides. Valence electron density (VED) is defined as the total number of valence electrons divided by volume per unit cell which is an important factor for analyzing the super hard materials. The calculated ground state properties like lattice constants *a, c* (Å), cell volume V_0(Å^3), valence electron density ρ(electrons/Å^3),bond-length RE-N (Å), Cohesive energy E_{coh} (eV), bulk modulus B_0 (GPa) and its derivative B_0' for the normal and high pressure structures of GdN, DyN and HoN are listed in

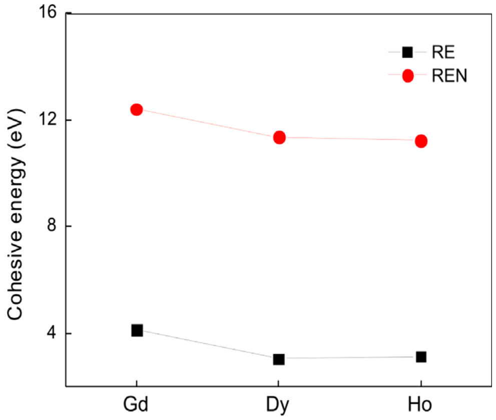

Fig. 1. Cohesive energies of rare earth metals (RE) and the corresponding nitrides in their stable structure.

Table 1
Calculated lattice parameters *a*,*c* (Å), cell volume V_0 (Å^3), the shortest RE–N bond distance (Å),Valence electron density ρ (electrons/Å^3), Cohesive energy E_{coh}(eV), bulk modulus B_0(GPa) and its derivative B_0'

	Work	GdN		DyN		HoN	
		NaCl	Wurtzite	NaCl	CsCl	NaCl	CsCl
V_0	Present work	31.24	28.38	29.41	30.37	29.02	32.16
a	Present work	4.997	2.97	4.901	3.12	4.878	3.18
	Exp.	4.988[a],4.974[b]		4.905[b]		4.874[b]	
	Theoretical	4.940[c]		4.874[c]		4.851[c]	
c	Present work		5.438				
ρ	Present work	0.480	0.528	0.578	0.559	0.620	0.559
RE-N	Present work	2.82	2.78	2.79	2.85	2.83	2.97
E_{coh}	Present work	12.40	10.12	11.35	9.43	11.23	9.25
B_0	Present work	201	114	123	81	138	98.5
	Exp.	192 ± 35[d]					
	Theoretical			121[c]		138[c],137.6[e]	
B_0'	Present work	3.45	4.06	3.5	3.68	3.78	4.02

[a] Exp, Ref. [8].
[b] Exp, Ref. [11].
[c] GGA, Ref. [14].
[d] Exp, Ref. [13].
[e] inter-ionic potential theory, Ref. [17].

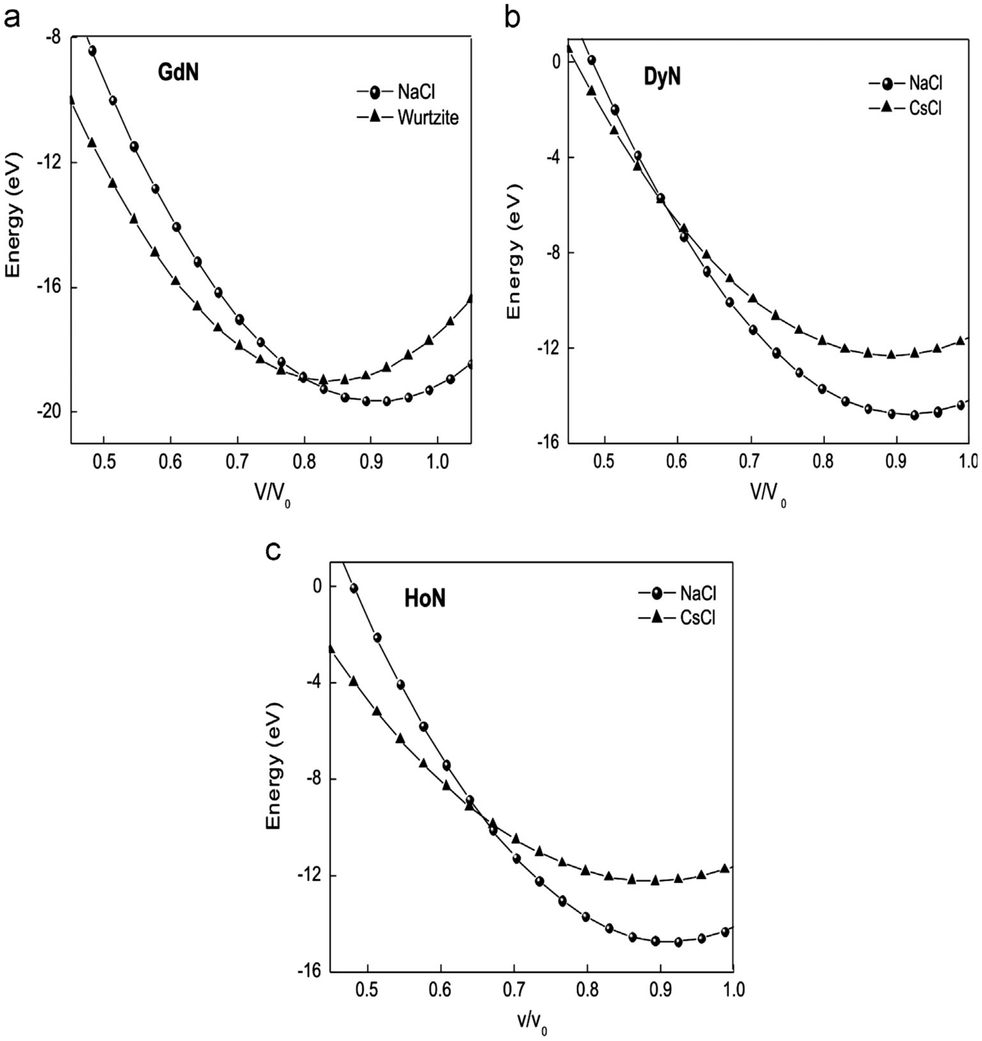

Fig. 2. Total energy (in eV) versus reduced volume for the normal and high pressure structures: (a) GdN, (b) DyN and (c) HoN.

Table 1 and are compared with the available experimental [8,11,13] and previous theoretical results [14,17]. From Table 1, it is found that the calculated ground state properties are in good agreement with the experimental and previous theoretical results. From Table 1, it is observed that, among the considered rare earth nitrides cubic HoN have the highest VED.

3.2. Structural phase transition under pressure

The total energy is calculated for the normal and high pressure phases of gadolinium nitride (GdN), dysorbium nitride (DyN) and holmium nitride (HoN) for different reduced volumes. The calculated total energies are plotted as a function of reduced volume and are given in Fig.2 (a–c). From Fig.2 (a–c), it is observed that all the three rare earth nitrides are stable in the NaCl phase at ambient pressure. On further reducing the volume, GdN undergoes structural phase transition from NaCl to wurtzite phase, whereas in DyN and HoN the structural phase transition is from NaCl to CsCl phase.

In order to observe these transitions in a more accurate manner, we have calculated the enthalpy using the formula

$$H = E + PV \tag{2}$$

where E is the total energy in eV and P represents the pressure (GPa) corresponding to a particular volume V (Å^3). The transition pressure value is determined by the intersection of enthalpy versus pressure curve and is presented in Fig. 3(a–c). From Fig. 3(a–c), it is found that the transition pressures are 18.2 GPa (NaCl→wurtzite), 104 GPa (NaCl→CsCl) and 138 GPa (NaCl→CsCl) for GdN, DyN and HoN respectively. The calculated transition pressures for GdN and HoN are consistent with the previous results of Abdelouahed and Alouani [16] and Bhajanker et al. [17]. So far, no experimental work on structural phase transition has been performed in these nitrides.

3.3. Electronic structure

The spin dependant band structures of GdN, DyN and HoN in the NaCl phase at normal pressure is calculated along various symmetry lines using GGA+U^{SIC} method and is given in Fig.4. Fig. 4 shows that GdN, DyN and HoN have very similar band structures at ambient pressure. From Fig. 4, it is found that in the majority spin channel, the lowest band around -5 eV is due to the 6s like states of the rare earth atom RE (RE=Gd,Dy, Ho) and the next lower state is due to the s-like states of the nitrogen atom, which lies around -12 eV. The energy bands in the valence state, just below the Fermi level (E_F) in the range of -2.98 eV to 0 eV, arise due to N-2p like states. Also the energy bands due to the 4f state electrons of the rare earth atom RE (RE=Gd, Dy, Ho) is present at the Fermi level (cluster of solid lines), which hybridize with the 2p state electrons of the nitrogen atom. Therefore it can be concluded that at ambient pressure, the majority spin states are completely filled and are found to exhibit metallic

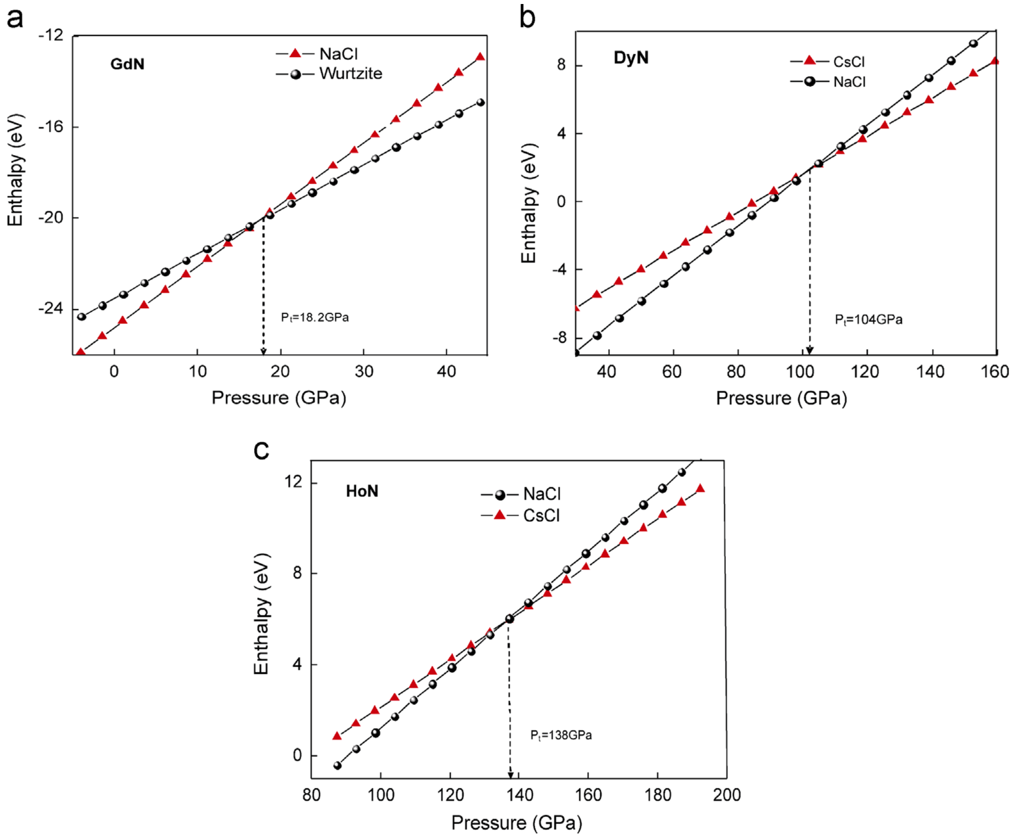

Fig. 3. Enthalpy versus pressure curve for the normal and high pressure structures: (a) GdN, (b)DyN and (c) HoN.

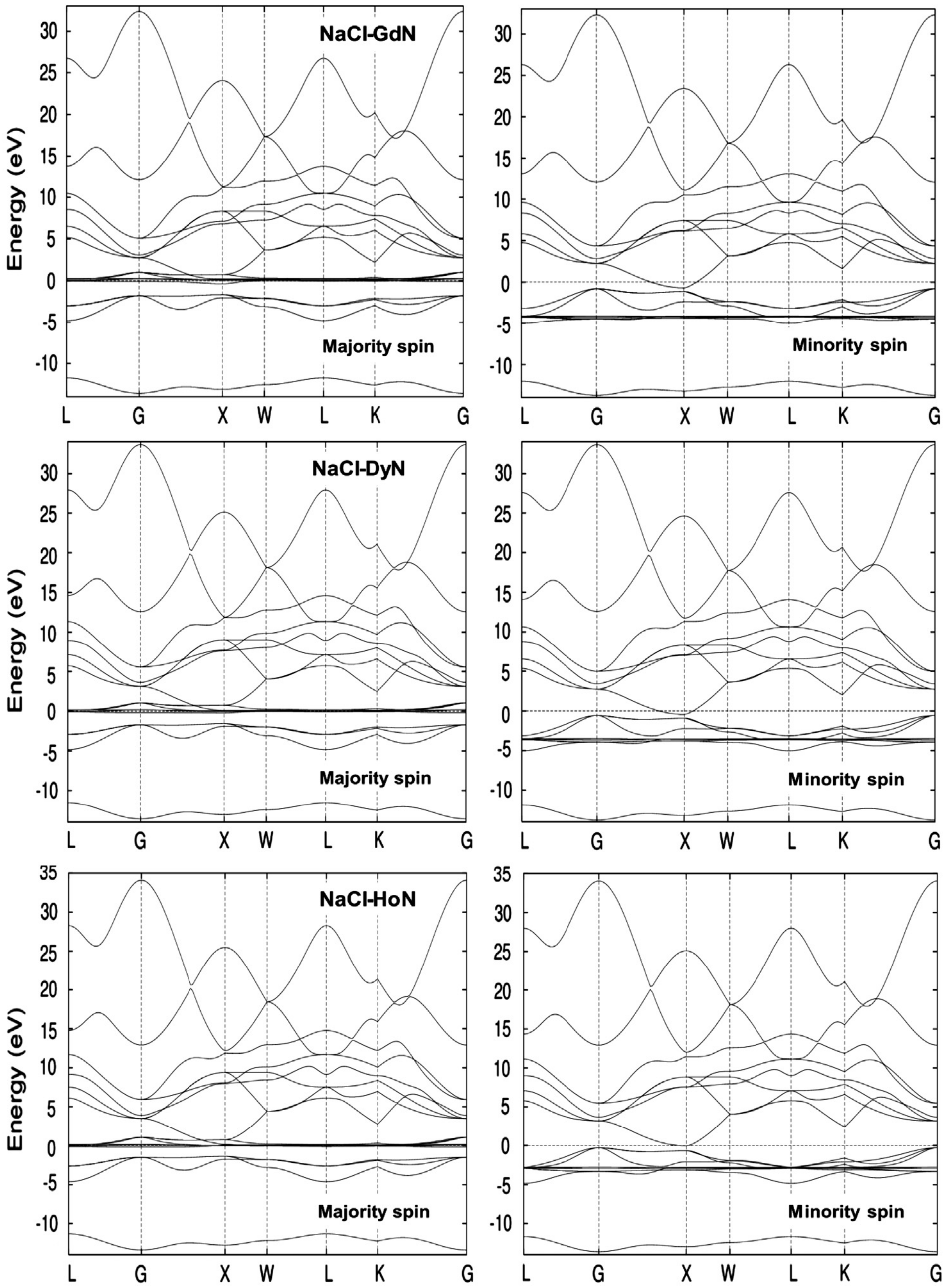

Fig. 4. Energy band structure along the principal high-symmetry directions in the Birllouin zone for the majority and minority spin of GdN, DyN and HoN in the stable NaCl structure.

character. On the other hand for the minority spin channel, a direct band gap around the Fermi level of about 0.98 eV, 0.95 eV and 1.05 eV at the X point is observed in GdN, DyN and HoN respectively. The estimated band gap is in good agreement with the experimental result of Hulliger [7].Hence, at normal pressure, all the three rare earth nitrides are half metallic ferromagnets.

The total density of states (DOS) of GdN, DyN and HoN for both the spin channels are given in Fig. 5(a–c). From the total DOS, it is observed that the peak due to 2s state electrons of the nitrogen atom is present at an energy range of ~ -12 eV. In the majority spin channel, the highest spike at the Fermi level is due to the 4f state electrons of the rare earth atom. The spikes, just below the Fermi level are mainly due to the N-2p states along with a small contribution from RE-4f states. Therefore at normal pressure, the majority spin state is metallic in nature. On the other hand, in the minority spin channel, the rare earth 4f states are present below the Fermi level and hybridize with the 2p states electrons of the nitrogen atom. This hybridization leads to a semiconducting behavior for the minority spin. Therefore it is concluded that, GdN, DyN and HoN are half-metallic ferromagnets at ambient pressure.

Under high pressure both DyN and HoN undergoes structural phase transition from sixfold co-ordinated NaCl structure to eight fold co-ordinated CsCl structure whereas GdN undergoes structural phase transition from sixfold co-ordinated NaCl

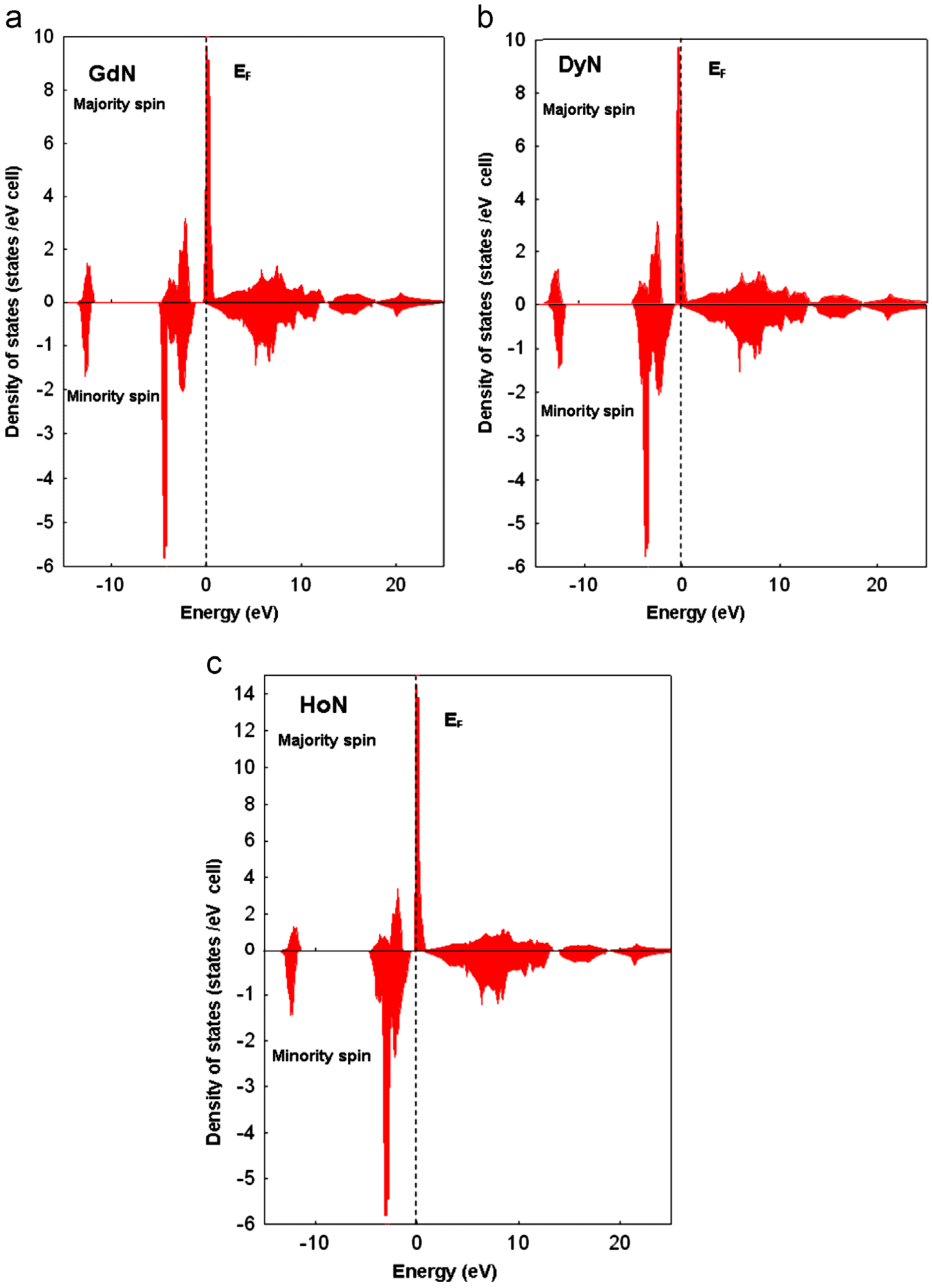

Fig. 5. Spin dependant total density of states (DOS) of GdN, DyN and HoN in the stable NaCl structure.

structure to hexagonal structure. Hence the high pressure band structure and density of states are computed with the CsCl structure as the stable structure for DyN and HoN and wurtzite as the stable structure for GdN. The high pressure band structure and density of states of GdN (wurtzite), DyN (CsCl) and HoN (CsCl) at their corresponding metallization pressure are given in Fig. 6 and Fig. 7(a–c) respectively. As pressure increases, no visible changes are observed in the majority spin whereas in the minority spin channel the distance of separation between the top of the valence band and bottom of the conduction band decreases. The main reason behind the metallic behavior of the minority spin case is due to the presence of energy bands at the Fermi level, which are formed due to the 2p state electrons of the nitrogen atom. Finally we observe half metallic to metallic transition in GdN, DyN and HoN at a pressure of 73.18 GPa ($V/V_0=0.72$), 118 GPa ($V/V_0=0.58$) and 141 GPa ($V/V_0=0.6$) respectively.

The covalent characteristics between the rare earth and N atoms can be confirmed by the charge density distribution. The charge density distribution for Cubic NaCl GdN,DyN and HoN is shown in Fig. 8(a–c). It is clearly seen that charge strongly accumulates between rare earth (RE) and N atoms, which means that a strong directional bonding exists between them. The bonding nature of these materials is found to be covalent-like due to the hybridization of N and rare earth atoms, but there is also some ionic character with electron

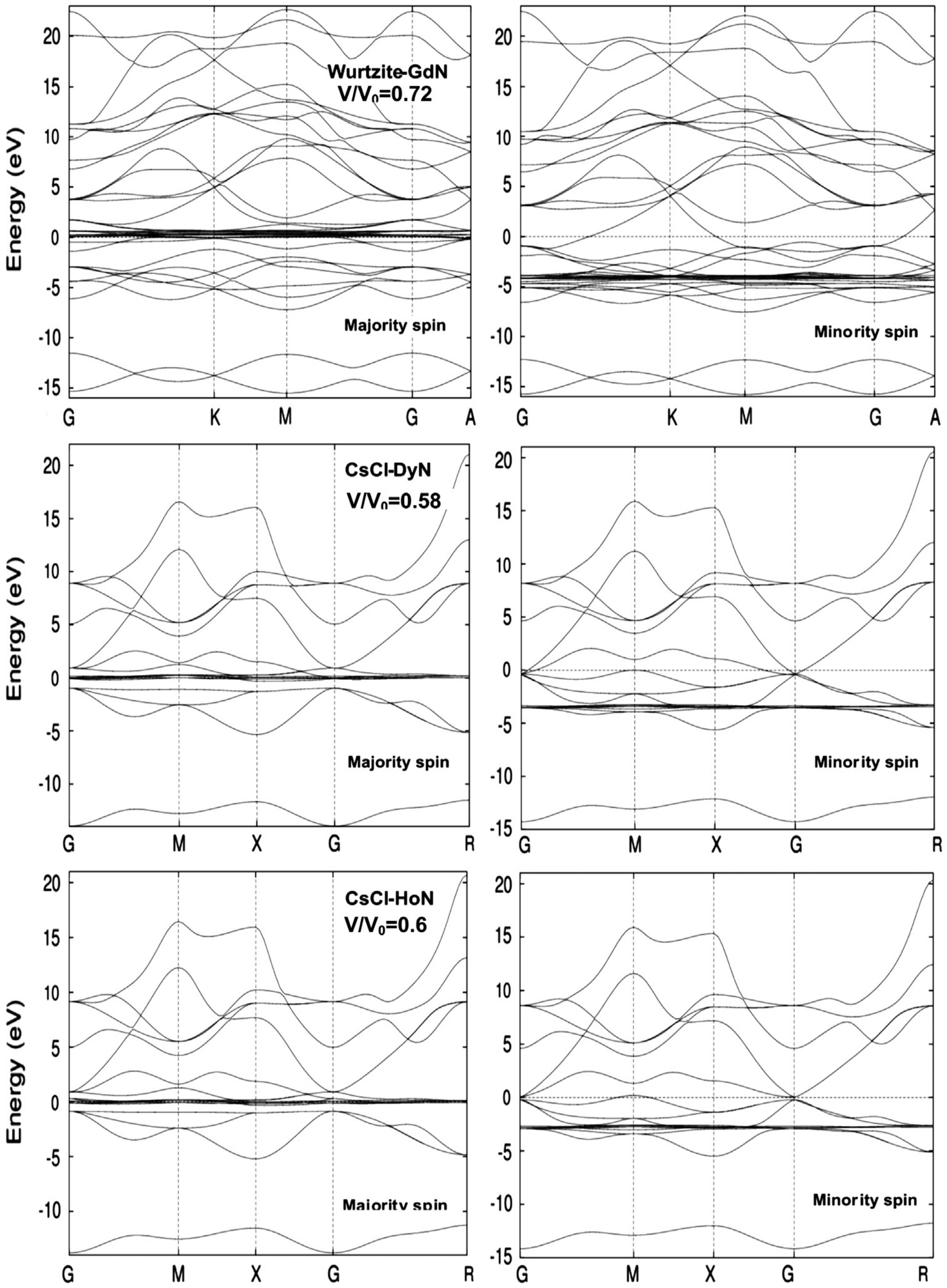

Fig. 6. Spin dependent band structure of GdN, DyN and HoN in the high pressure structure.

transfer from the rare earth to nitrogen atoms. Thus, our results demonstrate that the bonding is a mixture of covalent and ionic in nature.

3.4. Elastic properties

Elastic constants are the measure of the resistance of a crystal to an externally applied stress. For small strains Hooke's law is valid and the crystal energy E is a quadratic function of strain [27]. Thus to obtain the total minimum energy for calculating the elastic constants to second order, a crystal is strained and all the internal parameters are relaxed. Consider a symmetric 3×3 nonrotating strain tensor ε which has matrix elements ε_{ij} ($i,j=1,2$ and 3) defined by Eq. (3)

$$\varepsilon=\begin{pmatrix} e_1 & \frac{e_6}{2} & \frac{e_5}{2} \\ \frac{e_6}{2} & e_2 & \frac{e_4}{2} \\ \frac{e_5}{2} & \frac{e_6}{2} & e_3 \end{pmatrix} \tag{3}$$

such a strain transforms the three lattice vectors defining the unstrained Bravais lattice $\{a_K,\ K=1,2$ and 3$\}$ to the strained vectors$\{\ a'_K\ K=1,2$ and 3$\}$ as given by

$$a'_K=(I+\varepsilon)a_K \tag{4}$$

where I is defined by its elements, $I_{ij}=1$ for $i=j$ and 0 for $i\neq j$. Each lattice vector a_k or a'_k is a 3×1 matrix. The change in

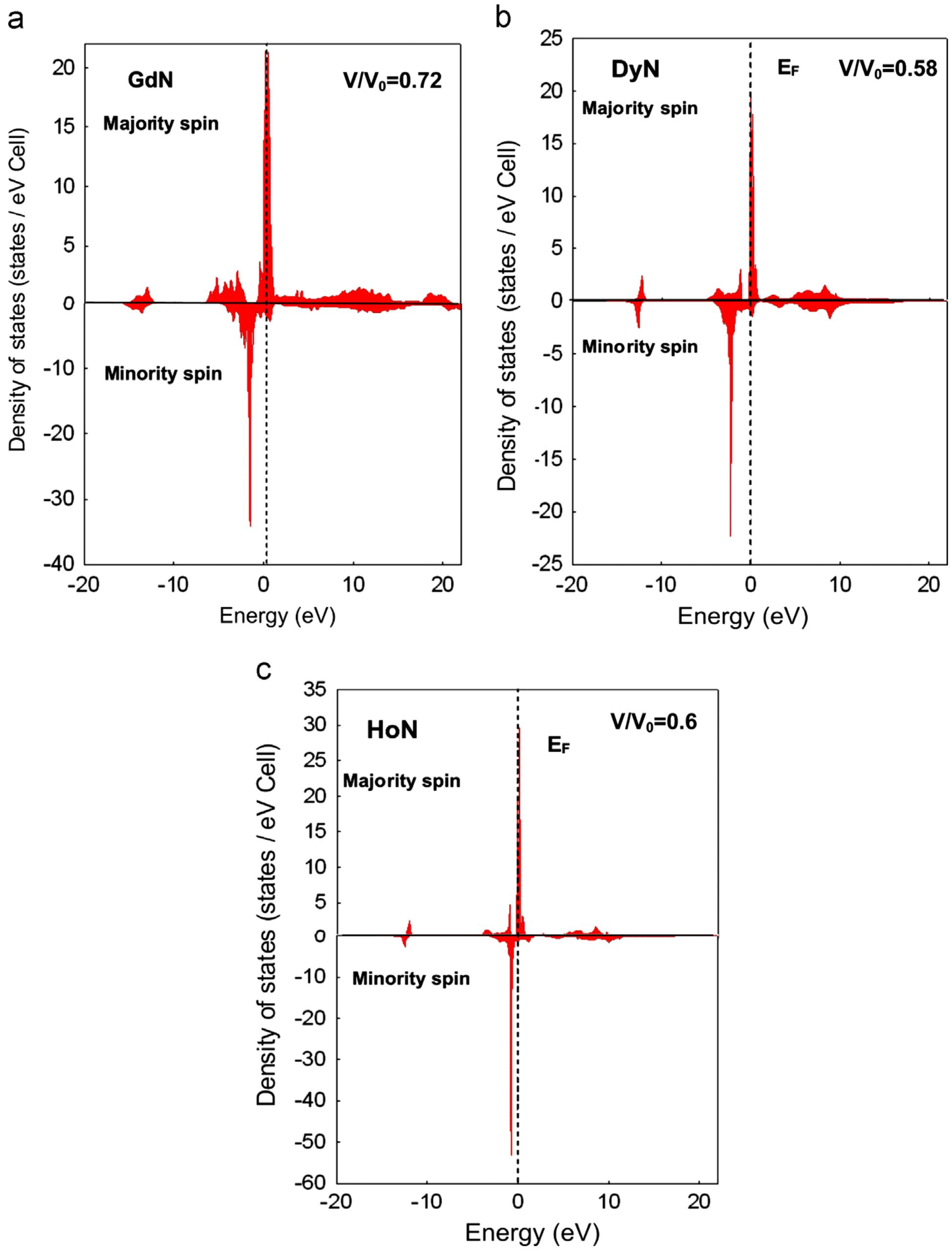

Fig. 7. Spin dependant total density of states (DOS) of GdN, DyN and HoN in the stable high pressure structure.

total energy due to the above strain (1) is

$$\Delta E=\frac{E(\{e_i\})-E_0}{V_0}=\left(1-\frac{V}{V_0}\right)P(V_0)+\frac{1}{2}\left(\sum_{1}^{6}\sum_{1}^{6}C_{ij}e_ie_j\right)+O\left(\{e_i^3\}\right) \tag{5}$$

where V_0 is the volume of the unstrained lattice, E_0 is the total minimum energy at this unstrained volume of the crystal, $P(V_0)$ is the pressure of the unstrained lattice, and V is the new volume of the lattice due to strain in Eq. (3). In Eq. (5), $C_{ij}=C_{ji}$ due to crystal symmetry. This reduces the elastic constants from 36 to 21. Further crystal symmetry reduces the number to 5 (C_{11}, C_{12}, C_{44}, C_{13}, C_{33}) for hexagonal crystals and 3(C_{11}, C_{12}, C_{44}) for cubic crystals. A proper choice of the set of strains $\{e_i,\ i=1,2,\ldots\ldots,6\}$, in Eq. (5) leads to a parabolic relationship between $\Delta E/V_0$ ($\Delta E\equiv E-E_0$) and the chosen strain. Such choices for the set $\{e_i\}$ and the corresponding form for ΔE are shown in Table 2 for cubic [28] and hexagonal [29] lattices. For each lattice structure of GdN,DyN and HoN studied, we strained the lattice by 0%, ±1%, and ±2% to obtain the total minimum energies $E(V)$ at these strains. These energies and strains are fitted with the corresponding parabolic equations of $\Delta E/V_0$ as given in Table 2 to yield the required second-order elastic constants. While computing these energies all atoms are allowed to relax with the cell shape and volume fixed by the choice of strains $\{e_i\}$. From the calculated C_{ij} results, the bulk modulus (B_0) and shear modulus (G) for the cubic and hexagonal crystals are calculated using the Voigt–Reuss–Hill (VRH) averaging scheme [30–32]. The strain energy $1/2C_{ij}e_ie_j$ of a given crystal in Eq. (5) must always be positive for all possible values of the set $\{ei\}$; otherwise the crystal would be mechanically unstable.

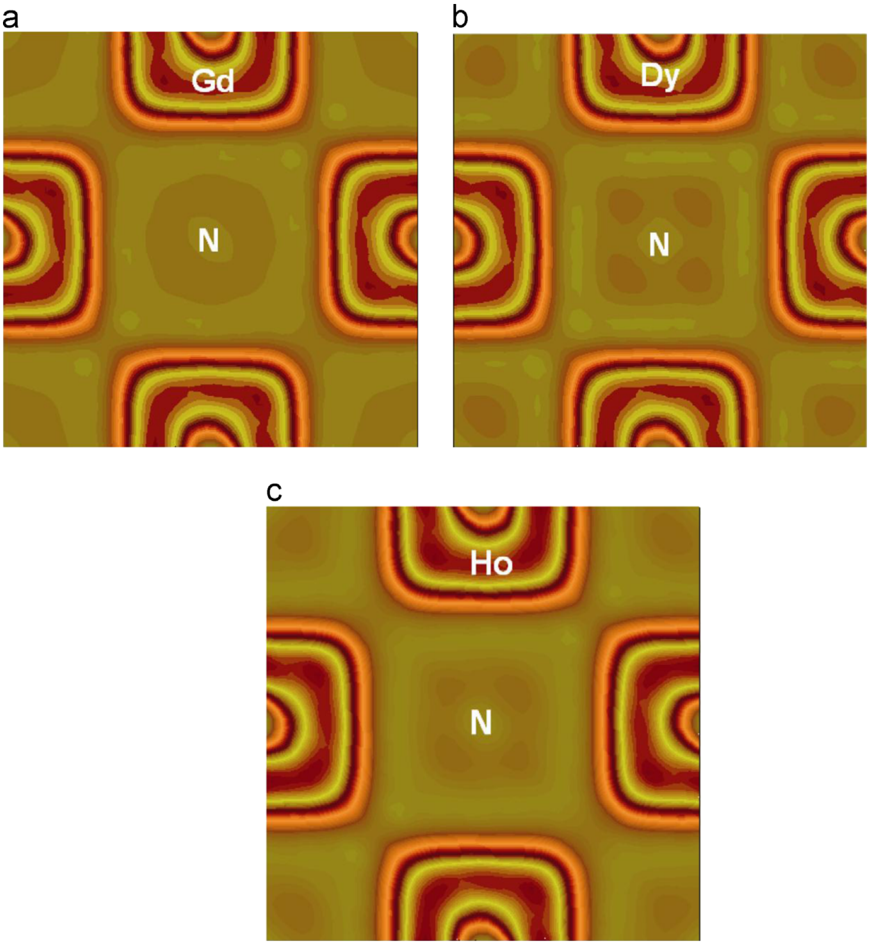

Fig. 8. Electronic charge density for: (a) GdN, (b)DyN and (c) HoN in the rocksalt structure.

Table 2
Strain combinations in the strain tensor [Eq.(5)] for calculating the elastic constants of cubic and hexagonal structures. The independent elastic constants for cubic (NaCl and CsCl structures) and hexagonal (Wurtzite structure) are calculated from the above strains. Symmetry dictates $C_{ij}=C_{ji}$ and all unlisted $C_{ij}=0$. The strain δ is varied in steps of 0.01 from $\delta=-0.02$ to 0.02. ΔE [Eq.(5)] is the difference in energy between that of the strained lattice and the unstrained lattice. The equilibrium or unstrained lattice volume is V_0.

Cubic crystals			Hexagonal crystals	
Strain	Parameters (unlisted $e_i=0$)	$\Delta E/V_0$	Parameters (unlisted $e_i=0$)	$\Delta E/V_0$
1	$e_1=e_2=\delta$, $e_3=(1+\delta)^{-2}-1$	$3(C_{11}\text{-}C_{12})\delta^2$	$e_1=\delta$	$(1/2)\ C_{11}\delta^2$
2	$e_1=e_2=e_3=\delta$	$(3/2)(C_{11}+2C_{12})\delta^2$	$e_3=\delta$	$(1/2)\ C_{33}\delta^2$
3	$e_6=\delta$, $e_3=\delta^2(4-\delta^2)^{-1}$	$(1/2)C_{44}\delta^2$	$e_4=\delta$	$(1/2)C_{44}\delta^2$
4			$e_1=e_2=\delta$	$(C_{11}+C_{12})\delta^2$
5			$e_1=e_3=\delta$	$(1/2)\ (C_{11}+C_{33}+2C_{13})\ \delta^2$

The calculated elastic constants C_{ij}(GPa),Young's modulus E(GPa), Shear modulus *G*(GPa), *B*/*G* ratio, elastic anisotropy factor A, Poisson's ratio (ν) and micro hardness *H*(GPa) are given in Table 3. From Table 3, it is found that the calculated elastic constants are in good agreement with the available data [14,17].

For a stable cubic structure, the three independent elastic constants C_{ij} (C_{11},C_{12}, C_{44}) should satisfy the Born–Huang criteria [33].

$$C_{44}>0,\ C_{11}>|C_{12}|,\ C_{11}+2C_{12}>0 \tag{6}$$

while for a hexagonal structure, the five independent elastic constants C_{ij} (C_{11},C_{12},C_{33},C_{13},C_{44}) should satisfy the well known Born–Huang criteria for stability [33].

$$C_{12}>0,\ C_{33}>0,\ C_{11}>C_{12},\ C_{44}>0 \tag{7}$$

Clearly, the calculated elastic constants for cubic NaCl, CsCl phases and hexagonal wurtzite phase of GdN, DyN and HoN satisfy Born–Huang criteria, suggesting that they are mechanically stable at ambient pressure. Young's modulus (E) and Poisson's ratio ν are the two important factors for technological and engineering application. The Young's modulus *E* is calculated using the

Table 3
Calculated Elastic constants C_{ij}(GPa), Young's modulus E(GPa), Shear modulus G(GPa), B/G ratio, Poisson's ratio ν, elastic anisotropy factor A and hardness H (GPa) for the normal and high pressure structures of GdN, DyN and HoN.

	Work	GdN		DyN		HoN	
		NaCl	Wurtzite	NaCl	CsCl	NaCl	CsCl
C_{11}	Present work	365	295	218	137	270	169
	Theoretical	201[a]		216[a]		399[a],270[b]	
C_{12}	Present work	119	123	76	53	72	63
	Theoretical	65[a]		65[a]		7[a],71[b]	
C_{44}	Present work	81	148	72	49	69	51
	Theoretical	83[a]		101[a]		101[a],70[b]	
C_{13}	Present work		30				
C_{33}	Present work		310				
E	Present work	266	137	180	141	203	133
G	Present work	104	53	72	46	81	52
ν	Present work	0.24	0.3	0.25	0.27	0.21	0.29
	Theoretical	0.245[a]		0.253[a]		0.018[a], 0.38[b]	
B/G	Present work	1.93	2.15	1.70	2.67	1.70	1.78
A	Present work	0.73		1.15		0.69	
H	Present work	15.34		12.0		11.42	

[a] GGA, Ref. [14].
[b] inter-ionic potential theory, Ref. [17].

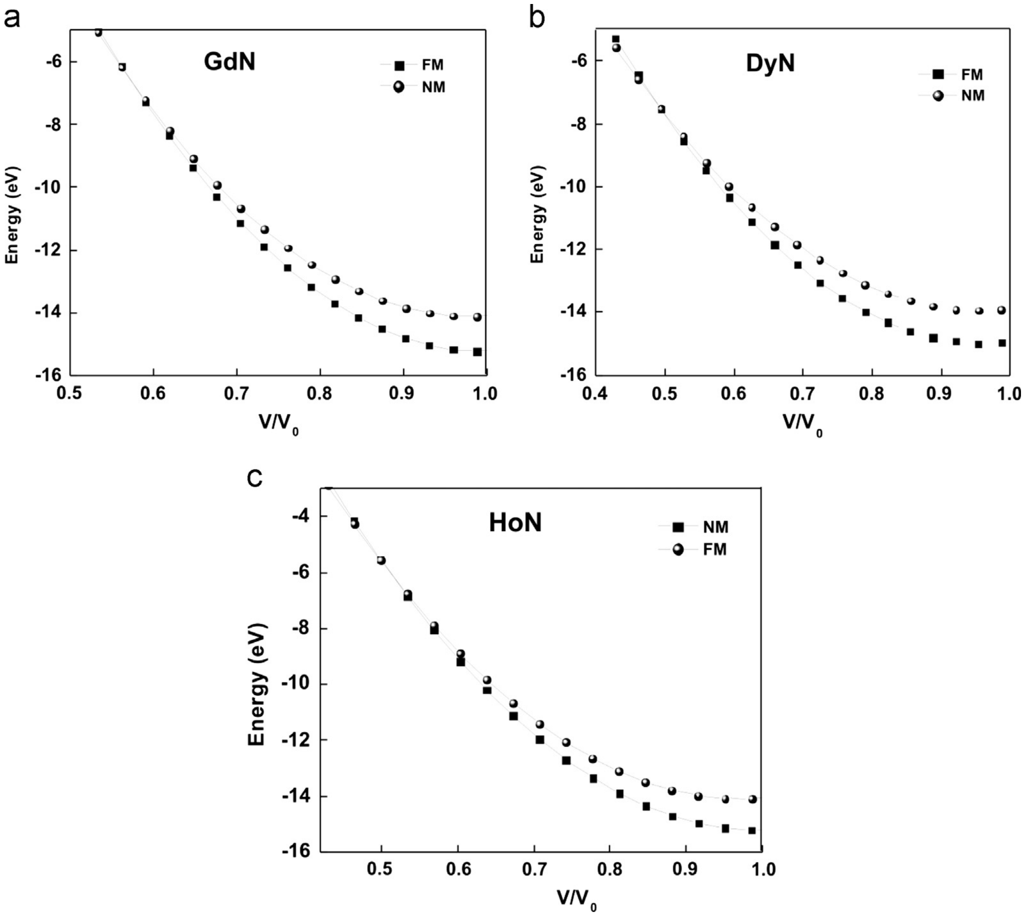

Fig. 9. Variation of total energy with relative volume in ferromagnetic (FM) and non-magnetic (NM) states of: (a) GdN, (b) DyN and (c) HoN in the NaCl structure.

following expression:

$$E = \frac{9BG}{(3B+G)} \tag{8}$$

The stiffness of the solid can be analyzed using the young's modulus (E) value. The larger the value of E, stiffer the material. The Young's modulus of GdN is higher than that of DyN and HoN. Therefore it is concluded that GdN is the stiffest material among the considered rare earth nitrides. Poisson's ratio is associated with the volume change during uniaxial deformation, which is expressed as

$$\nu = \frac{C_{12}}{C_{11} + C_{12}} \tag{9}$$

During elastic deformation no volume change occurs, if $v=0.5$ and this indicates that the material is incompressible. The low v value means that a large volume change is associated with its deformation. In addition, Poisson's ratio provides more information about the characteristics of the bonding forces than any of the other elastic constants. Among the three rare earth nitrides, the Poisson's ratio of HoN is lower than GdN and DyN, indicating that the Ho–N bonding is more directional in nature.

A high B/G value is associated with ductility, while a low B/G value represents brittleness. The critical value which separates ductile and brittle materials is about 1.75. From Table 3, it is found that GdN, DyN and HoN are brittle. For cubic phase; the anisotropy factor is defined as

$$A = \frac{2C_{44}}{C_{11} - C_{12}} \tag{10}$$

The value of $A=1$ represents completely elastic isotropy, while values smaller or larger than one measure the degree of elastic anisotropy. It can be seen from Table 3 that GdN,DyN and HoN are elastically anisotropic.

3.5. Magnetic phase transition

Non-spin and spin polarized calculations are performed to obtain total energies of cubic NaCl phase of RENs (RE: Gd, Dy,Ho) by using VASP code. The variation of total energy (per formula unit) with relative volume in ferromagnetic (FM) and non-magnetic (NM) state is given in Fig. 9(a–c), to check the magnetic stability of cubic NaCl structured rare earth nitrides RENs (RE: Gd, Dy,Ho) at normal pressure. From the calculations it is found that all the three nitrides are stable in the FM state in the NaCl structure at normal pressure. The calculated magnetic moment of cubic NaCl phase of RENs (RE: Gd, DY, Ho) are summarized in Table 4. From Table 4, it is found that the contribution to the magnetic moment is entirely from the rare earth atom rather than N atom. The calculated values of magnetic moments of the rare earth nitrides are compared with the available experimental [12] and previous theoretical results [15,19], which reveal good agreement. The variation of magnetic moment with pressure for GdN, DyN and HoN is given in Fig. 10(a–c). Fig. 10(a–c) depicts a magnetic phase transition from ferromagnetic (FM) to non-magnetic (NM) state at a pressure of 252 GPa, 242 GPa and 236.7 GPa for GdN, DyN and HoN respectively. The main reason behind this magnetic transition is magnetic collapse due to band widening in lanthanide metal ions under pressure.

4. Conclusion

In conclusion, first principles calculations have been performed using Vienna ab-initio simulation code to investigate the structural, electronic, magnetic and mechanical properties of GdN, DyN and HoN with the normal (NaCl) and high pressure (wurtzite, CsCl) structures. The calculated ground state properties are in good agreement with the available experimental and previous theoretical results. Our results suggest that cubic NaCl structure is the most stable structure at ambient pressure. We have also predicted a structural phase transition from NaCl to wurtzite phase in GdN and from NaCl to CsCl phase for DyN and HoN at high pressure. Electronic structure reveals that cubic NaCl GdN,DyN and HoN are half-metallic ferromagnets with a direct band gap of 0.98 eV,

Table 4
Magnetic moment of RENs (RE: Gd, Dy, Ho) in units of μ_B.

Structure	Work	GdN	DyN	HoN
Total	Present work	6.921	5.000	3.999
	Exp.	7.0[a]		
	Theoretical	6.93[b],7.0[c]	4.95[b],5.0[c]	3.95[b],4.0[c]
RE		6.774	4.944	3.9
N		0.147	0.117	0.189

[a] Exp, Ref. [12].
[b] LSDA, Ref. [15].
[c] SIC-LSD, Ref. [19].

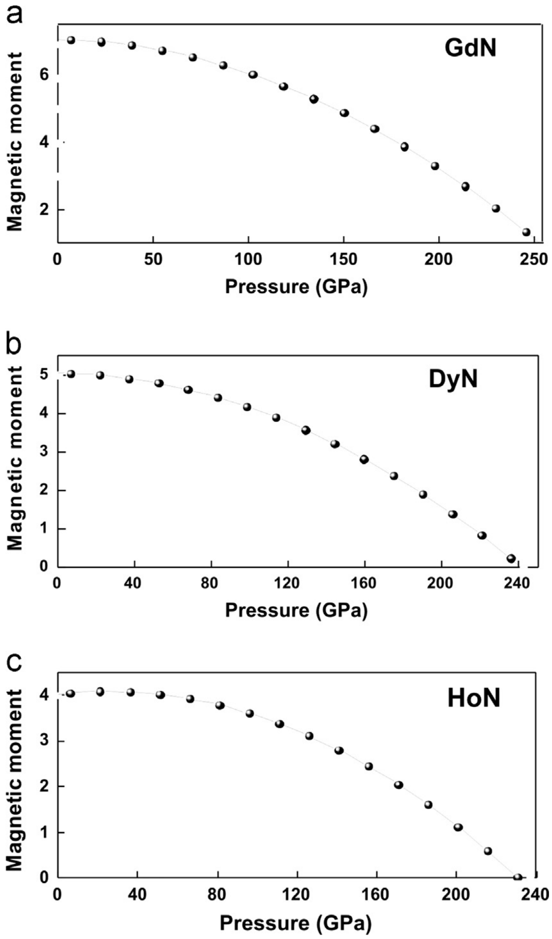

Fig. 10. Variation of magnetic moment of: (a) GdN, (b) DyN and (c) HoN in the NaCl structure.

0.95 eN and 1.05 eV respectively. The calculated band gap is in good agreement with the experimental data. As pressure increases, we observe half metallic to metallic transition in GdN, DyN and HoN at a pressure of 73.18 GPa, 118GPa and 141GPa respectively. The bonding nature of these materials is found to be covalent-like due to the hybridization of N and metal atoms, but there is also some ionic character with electron transfer from the metal to nitrogen atoms. The calculated elastic constants obey the necessary mechanical stability conditions suggesting that all the nitrides are mechanically stable in both the normal (NaCl) and high pressure (wurtzite and CsCl) structures. On further increasing the pressure, we also observe ferromagnetic (FM) to non-magnetic (NM) transition at 252 GPa, 242 GPa and 236.7 GPa for GdN,DyN and HoN respectively.

Acknowledgment

We thank our college management for their constant encouragement. The financial assistance from UGC under Research Award Scheme [No. F: 30–36 /2011 SA-II], India is duly acknowledged with thanks.

References

[1] G. Pagare, P. Soni, V. Srivastava, Sanyal P Sankar, High-pressure behavior and elastic properties of heavy rare-earth Gd monopnictides, Journal of Physics and Chemistry of Solids 70 (2009) 650.

[2] I.N. Yakovkin, T. Komesu, P.A Dowben, Band structure of strained Gd (0001) films, Physical Review B 66 (2002) 035406.

[3] H.M. Liu, C.Y Ma, C Zhu, J-M Liu, Strain induced ferroelectricity in GdN: first-principles calculations, Journal of Physics: Condensed Matter 23 (2011) 245901.

[4] E. Kaldis, G.V Schulthess, P. Wachter, Electrical resistivity of anti-ferromagnetic GdP, Solid State Communications 17 (1975) 1401.

[5] R.A. de Groot, F.M. Mueller, P.G. Van Engen, K.J.H. buschow, New class of materials: half-metallic ferromagnets, Physical Review Letters 50 (1983) 2024.

[6] Chun-Gang Duan, R.F. Sabirianov, W.N. Mei, P.A. Dowben, S. S. Jaswal, E.Y. Tsymbal, Electronic, magnetic and transport properties of rare-earth monopnictides, Journal of Physics: Condensed Matter 19 (2007) 315220.

[7] F. Hulliger, in: Karl A. Gschneider Jr., LeRoy Eyring (Eds.), Handbook on the Physics and Chemistry of Rare Earths, 4, Norht-Holland Physics Publishing, New York, 1979, pp. 153–236.

[8] R.C. Brown, N.J. Clark, Composition limits and vaporization behaviour of rare earth nitrides, Journal of Inorganic and Nuclear Chemistry 36 (1974) 2507.

[9] D.X. Li, Y. Haga, H. Shida, T. Suzuki, Magnetic properties of ferromagnetic GdN, Physica B 199 (1994) 631.

[10] D.X. Li, Y. Haga, H. Shida, T. Suzuki, Y.S. Kwon, G. Kido, Magnetic properties of stoichiometric Gd monopnictides, Journal of Physics: Condensed Matter 9 (1997) 10777.

[11] U. Essen, W. Klemm, Zur Kenntnis der Nitride der Cererden, Zeitschrift für Anorganische und Allgemeine Chemie 317 (1962) 25.

[12] W. Klemm, G. Winkelmann, Zur Kenntnis der Nitride der Seltenen Erdmetalle, Zeitschrift für Anorganische und Allgemeine Chemie 288 (1956) 87.

[13] D.B. Mc Whan, Effect of pressure on the Curie temperature and volume of GdN, Journal of Chemical Physics 44 (1966) 3528.

[14] Faming Jun Yang, Haiyan Gao, Huiyang Wang, Xianfeng Gou, Zhiping Hao, Li, Elastic properties and hardness calculations of lanthanide nitrides in rocksalt structure, Materials Chemistry and Physics 119 (2010) 499–504.

[15] P Larson, Walter R.L. Lamrecht, Electronic structure of rare-earth nitrides using the LSDA+U approach: Importance of allowing 4f orbitals to break the cubic crystal symmetry, Physical Review B 75 (2007) 045114.

[16] Samir Abdelouahed, M. Alouani, Calculated electronic properties and structural phase transitions of GdN pnictide under hydrostatic pressure, Physical Review B 76 (2007) 214409.

[17] Vipul Srivastava Sanjay Bhajanker, P Sankar, Sanyal, structural, mechanical and thermal properties of some Holmium Pnictides under pressure: a theoretical approach, Physica B 407 (2012) 2376.

[18] A Hasegawa, A. Yanase, Energy band structures of Gd-Pnictides, Journal of Physical Society of Japan 42 (1977) 392.

[19] C.M. Aerts, P Strange, M. Horne, W.M. Temmerman, Z Szotek, A. Svane, Half-metallic to insulating behaviour of rare-earth nitrides, Physical Review B 69 (2004) 045115.

[20] J.P. Perdew, S. Burke, Generalized gradient approximation for the exchange-correlation hole of a many-electron system, Physical Review B 54 (2004) 16533.

[21] P.E. Blöchl, Projector augmented-wave method, Physical Review B 50 (1994) 17953.

[22] G. Kresse, J. Joubert, From ultrasoft pseudopotentials to the projector augmented-wave method, Physical Review B 59 (1999) 1758.

[23] G. Kresse, J. Hafner, Ab initio molecular dynamics for liquid metals, Physical Review B 47 (1993) 558.

[24] G. Kresse, J. Furthmuller, Efficiency of ab-initio total energy calculations for metals and semiconductors using a plane-wave basis set, Computational Materials Science 6 (1996) 15.

[25] J.P. Perdew, S. Burke, Generalized gradient approximation made simple, Physical Review Letters 78 (1997) 1396.

[26] H.J Monkhorst, J.D. Pack, Special points for Brillouin-zone integrations, Physical Review B 13 (1976) 5188.

[27] J.F. Nye, Physical Properties of Crystals, Their Representation by Tensors and Matrices, Oxford Press, 1957 (Chap VIII).

[28] M. Kalay, H.H. Kart, T. Çagin, Elastic properties and pressure induced transitions of ZnO polymorphs from first-principle calculations, Journal of Alloys and Compounds 484 (2009) 431.

[29] A.T. Asvini meenaatci, R. Rajeswara palanichamy, K. Iyakutti, Electronic structure, structural stability, mechanical and superconducting properties of group VB nitrides, A First principles Study,Solid State Sciences 19 (2013) 36–44.

[30] W Voigt, Lehrbuch de Kristallphysik, Terubner, Leipzig, 1928.

[31] A Reuss, Berechnung der Fließgrenze von Mischkristallen auf Grund der Plastizitätsbedingung für Einkristalle.Z.Angew, Mathematics and Mechanics 9 (1929) 49.

[32] R Hill, The elastic behaviour of a crystalline aggregate, in: Proceedings of the Physical Society, London, Section A 65, 1952 p. 349.

[33] M. Born, K. Huang, in: Dynamical Theory of Crystal Lattices, Clarendon, Oxford, 1956.